DOI 10.1007/s11595-017-1652-4

Effects of Aging Temperature on Microstructure and High Cycle Fatigue Performance of 7075 Aluminum Alloy

YANG Dalian[1,2], LIU Yilun[2,3*], LI Songbai[2], MA Liyong[4], LIU Chi[2], YI Jiuhuo[2]

(1. Hunan Provincial Key Laboratory of Health Maintenance for Mechanical Equipment, Hunan University of Science and Technology, Xiangtan 411201, China; 2. School of Mechanical and Electrical Engineering, Central South University, Changsha 410083, China; 3. Light Alloy Research Institute, Central South University, Changsha 410083, China; 4. School of Mechanical Engineering, Hebei University of Architecture, Zhangjiakou 075051, China)

Abstract: The hardness, the tensile and the high-cycle fatigue (HCF) performances of 7075 aluminum alloy were investigated under temper T651, solution treated at 380 ℃ for 0.5 h and aged at different temperatures (150, 170, 190 ℃) for 10 hours. The optimal microstructures and the fatigue fracture surfaces were observed. The results show that the hardness and the tensile performances are at their optimum at T651, but the fatigue life is the shortest. The hardness and the elongation are the lowest after solution treatment. With the aging temperature increasing (150-190 ℃), the HCF is improved. The crack is initiated from the impurity particles on the subsurface. Treated at 170 ℃,the area of the quasi-cleavage plane and the width of parallel serrated sections of the crack propagation are the largest. With increasing aging temperature, the dimple size of finally fracture surfaces becomes larger and the depth deeper.

Key words: creep aging forming (CAF); high cycle fatigue (HCF); microstructure; 7075 aluminum alloy

1 Introduction

With the rapid development of modern industry, the high requirements of aerospace equipment accelerate the invention and the application of new manufacturing technologies, in which the creep age forming technology (CAF) is mainly to form wide large– contoured wing skins[1,2]. The CAF is a process that combines the effects of creep, stress relaxation and age hardening. Compared with the traditional forming technologies, such as the stretch forming (SF), the brake forming (BF), and the shot peening forming (SPF), CAF has more advantages[3,4].

Many researchers have done a lot of work on the application of the CFA technology. Sarioglu *et al*[5] and Brav *et al*[6] studied the fatigue crack growth behavior of the 2024 aluminum alloy under different aging conditions, and found that aging treatment can improve the fatigue performance. In addition, Jin *et al*[7] gave the similar conclusions based on their investigation; Zhan *et al*[8] investigated the hardness, the strength and the elongation of 2124 aluminum alloy under different aging conditions, and found that under conditions of stress aging, the strength was increased, but the plasticity was reduced; Zhu *et al*[9] studies the effects of the stress on the microstructure and performance of Al-2.5Cu, Al-4Cu and Al-5Cu alloy, and pointed out that the directional effect of the stress are affected by the size, the temperature and the alloy composition; Liu *et al*[10] studied the stress corrosion cracking (SCC) behavior and the strength properties of 7075 aluminum alloy with various tempers, and revealed that the hardness, the strength and the SCC susceptibility of 7075 aluminum alloy are greatly concerned with the aging time and the aging temperature; Zhu[11] reported the effects of the stretch rate on residual stress of the 7075 aluminum alloy sheet.

Despite comprehensive work, the effects of CAF on the high cycle fatigue (HCF) are less studied. In practice, fatigue fracture is the most common form of failure in most material and structure subject to low-stress cyclic loading. But the fatigue fracture is difficult

(Received: Oct. 20, 2016; Accepted: Feb. 17, 2017)

YANG Dalian (杨大炼): PH D; E-mail: hyydl216@163.com

*Corresponding author: LIU Yilun (刘义伦): Prof.; Ph D; E-mail: ylliu@csu.edu.cn

Funded by the National Natural Science Foundation of China (Nos. 51375500, and 51375162); Scientific Research Project of Hunan Province Department of Education(No.17C0886); Open Funded Projects of Hunan Provincial Key Laboratory of Health Maintenance for Mechanical Equipment(No.201605)

to detect and prevent because the plastic deformation is inconspicuous, therefore, it is significant to investigate the high cycle fatigue performance for the application of aluminum alloy.

During the CFA process, the aggravation of the precipitation and segregation of the early strengthening phase lead to the inhomogeneity of the composition, which is easy to cause stress concentration and crack initiation. The size, the distribution and the orientation of the precipitated phase affect the number, the location and the direction of the initiation cracks, which leads to the macro fatigue performance uncertainty. The temperature of CAF is an important parameter that affects the performances of the treated material[12]. With the increase of aging temperature, the creep rate increases. When the temperature drops, the intersection mechanism of the dislocation and the twin interface lead to the initiation and propagation of the cracks. Due to the randomness of the intersection of the dislocation and the twin interface, the macro fatigue performance of material also displays the randomness. The fatigue performance of material is controlled by the CAF process, therefore, it must be studied comprehensively. In this investigation, the 7075 aluminum alloy will be taken as the object. The microstructures, the hardness, the tensile performance, and the HCF performance of 7075 aluminum alloy will be investigated at different aging temperature to provide guidance for practical application and process improvement.

2 Experimental

2.1 Materials

The investigation was carried out on 7075 aluminum alloy plate, the thickness of which was 4 mm, treated with the T651 temper. 7075 aluminum alloy is a kind of alloy with high strength, and finds its wide applications in aviation aerospace industry. The chemical composition is given in Table 1.

Table 1 Chemical composition of 7075 aluminum alloy/wt%

Element	Ti	Mn	Si	Fe	Cr	Cu	Mg	Zn	Al
Content/ wt%	0.019	0.034	0.06	0.17	0.18	1.5	2.45	5.71	Bal.

2.2 Solution and aging treatments

The 7075 aluminum alloy plate was cut into samples with dimension 360 mm × 220 mm × 4 mm by wire electrical discharge machining (WEDM). The solution treatment was carried out at 480 ℃ for 30 min in the chamber type electric resistance furnace (SX-12-10), followed by quenching immediately in water (25 ℃), and the transfer time from the furnace to water was less than 5 seconds.

After solution treatment, some samples were aged. The aging treatments were conducted on a pair of dies with cylindrical surfaces, the radius of which was 1 500 mm. During the aging process, some screws and nuts were used to load the pre-tightening force. The 7075 aluminum alloy plates were aged at three temperature conditions (150, 170, 190 ℃) for 10 hours respectively. The experimental details are shown in Table 2.

Table 2 The experimental details

Test No.	Temper	Solution treatment		Aging treatment	
		Time/h	Temperature/℃	Time/h	Temperature/℃
C1	T651	-	-	-	-
C2	T651	0.5	480	-	-
C3	T651	0.5	480	10	150
C4	T651	0.5	480	10	170
C5	T651	0.5	480	10	190

2.3 Hardness, tensile and HCF tests

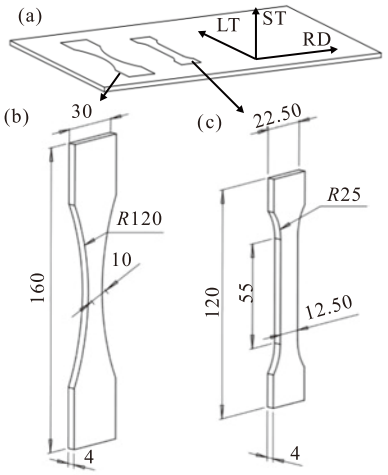

Fig.1 Specimens: (a) the position of the specimens in plate ;(b) HCF specimen; (c) tensile specimen. (unit: mm)

The HCF specimens and the monotonic tensile specimens were machined by WEDM along the direction shown in Fig.1 (a), and the shapes are shown in Fig.1 (b) and Fig.1 (c), respectively. The monotonic tensile test conforms to the specifications in ASTM E8M-2004[13]; and the high cycle fatigue test conforms to the specifications in ASTM E466-2007[14]. The stress axes of the specimens parallel to the long transverse direction (LT) and are perpendicular to the longitudinal rolling direction (RD). The specimen surfaces were polished by fine sandpaper in order to reduce the stress concentration. For the monotonic tensile tests, three specimens of each group were machined, for fatigue

life experiments, and fifteen specimens of each group were machined.

The hardness tests were conducted on a digital micro hardness tester (HVS-1000Z). A load of 1 kg was applied in the hardness measurements and the loading time was 30 s. Three indentations were made on each specimen and the average hardness values were calculated.

The monotonic tensile tests and the HCF tests were conducted on a fully-automated, closed-loop servo hydraulic materials test system which was made by the MTS Company of United States (MTS-50 kN). The load cell of the testing system had a capability of ±50 kN axial load. A high sensitive extensometer was used for the measurement of the strain in the gage section of the monotonic tensile specimens. The tensile speed was 2 mm/min. In HCF test program, the stress ratio R=0.1, sinusoidal load. The peak stress was 130 - 350 MPa. The loading frequency was 40 Hz. All tests were conducted at room temperature (25 ℃), in the air.

The fracture surfaces were observed by a scanning electron microscope (Tescan MorA3 Lmu) with an acceleration voltage 20 kV. The microstructural examination was carried out using an optical microscope (Leica DMI-5000M), and the etchant used in microscopic examination was Keller's reagent (2 mL HF (48%) + 3 mL HCl+ 5 mL HNO_3+ 190 mL H_2O).

3 Results and discussion

3.1 Effects of aging temperature on microstructure

Fig.2 presents the optical microstructure of the three batches of the materials used in the current investigation. Each stereography was synthesized from three microstructures taken on the sections perpendicular to the longitudinal rolling direction (RD), and the long transverse direction (LT) and the short transverse direction (ST).

It can be seen from Fig.2 that the grains are squashed along the ST direction and some of them were crushed. Moreover. The grains are elongated along direction LT and RD, and the fibrous grains are formed. As shown in Fig.2 (a), the boundaries of grains are clear and the sizes are even. Some impurity particles are observed. Those particles are harmful to improve the performance. The crack initiation results from the impurity particles. Inside the crystal grain, the nano-scale phase particles dispersively distribute, which has a positive effect on the material performance. After solution treatment (380 ℃+30 min), most of the second phase particles dissolve in the α-Al matrix, but a little of them are difficult to dissolve, as shown in Fig.2 (b). Recrystallization phenomenon occurs during the solution treatment, and the sizes of some recrystallizing grains are increased. As can be seen from Fig.2 (c) to Fig.2 (e), during aging forming treatment, the recrystallization phenomenon continues to occur. The second phase precipitates gradually under the stress and the temperature, the equiaxed grains can be observed. With increasing aging temperature, the grain size is refined and many precipitations distribute evenly inside the grains, which can improve the performance of the alloy.

3.2 Effects of aging temperature on tensile performance

Fig.3 shows the stress- strain curves of 7075 aluminum plate under different treatment conditions. As can be seen from Fig.3, the tensile curves of 7075 aluminum alloy have no obvious yield period. After the elastic deformation period, the plastic reinforcement period follows. After the peak stress, with increasing

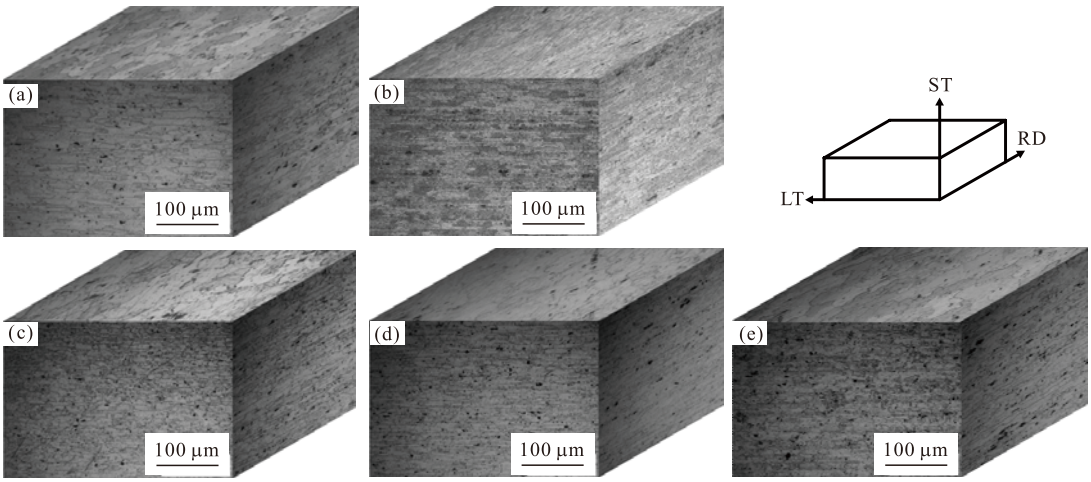

Fig.2 Optical microstructures of the three directions of the materials: (a): C1, (b): C2; (c): C3; (d): C4; (e): C4

strain, the material enters the necking down period and the stress decreases, then fracture subsequently excludes the curve of C2, without obvious necking down, after the peak stress, the material fractures quickly. It is shown that the plastic performance of the 7075 aluminum alloy decreases markedly after solution treatment.

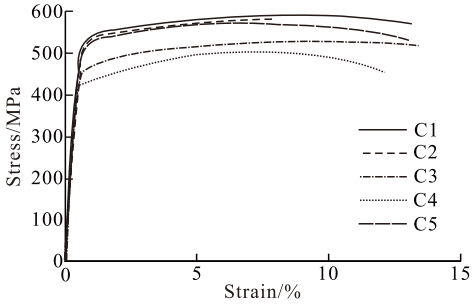

Fig.3 Uniaxial tensile stress-strain curves

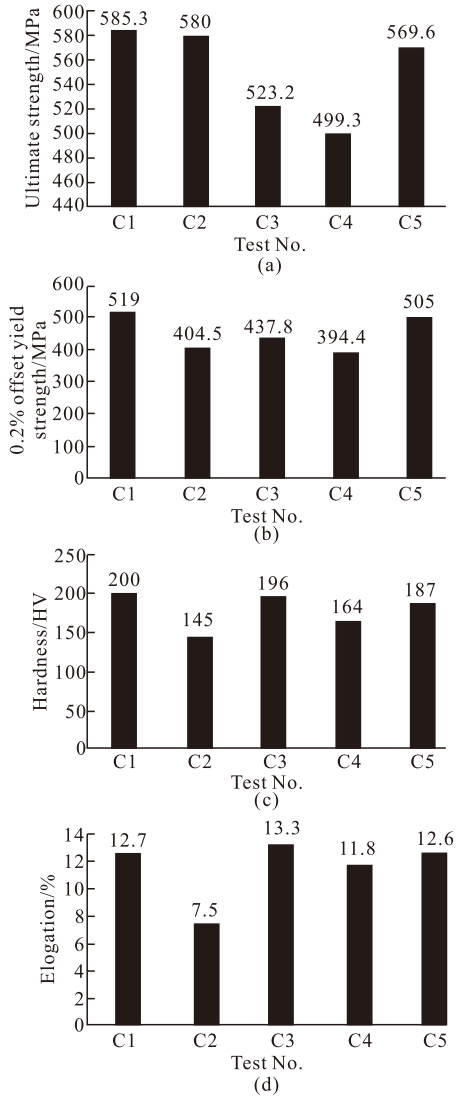

Fig.4 Results of uniaxial tensile test: (a) the ultimate strength; (b) the 0.2% offset yield strength; (c) the hardness; (d) the elongation

The ultimate strength, the 0.2% offset yield strength and the elongation of tests C1 to C5 are shown in Fig.4. It can be seen that the treatment conditions have great effects on the monotonic tensile performance. Test C1 has the highest ultimate strength 585.3 MPa and the highest 0.2% offset yield strength 519.0 MPa. The ultimate strength of test C2 decreases only a little, but the 0.2% offset yield strength and the elongation decrease obviously, by respectively 404.5 MPa and 7.5%. After aging treatment, both the ultimate strength and the 0.2% offset yield strength decrease but the elongation increases. The ultimate strength, the 0.2% offset yield strength and the elongation of test C4 (treated at 170 ℃ for 10 h) is the lowest, and test C3 (treated at 150 ℃ for 10 h) is lower, while test C5 (treated at 190 ℃ for 10 h) is the highest, close to 569.3 MPa, and the 0.2% offset yield strength near 505.0 MPa, with the elongation 12.6%, the tensile performance of test C5 is close to the tensile performance of test C1.

3.3 Effects of aging temperature on HCF

The load should be taken off if the cycles are over 10^{-7} because if the cycles are more than 10^{-7}, it is generally considered that the specimen survives forever under the stress level.

It is well known that the relationship between the cycles and the stress can be described by the S-N curve, usually, the test data are fit using empirical equations. The empirical equations include: (1) The exponential equation[15]; (2) The power equation[16]; (3) The Basquin equation[17]; and (4) The Weibull equation[18]. The exponential equation is a semi-logarithmic linear equation, while the power equation and the Basquin equation are only suitable for the case that the cycles are more than 10^7. The Weibull equation is a nonlinear equation in double logarithm coordinates. Therefore, in the current investigation, the Weibull equation is adopted to fit the SN curve. The expression is as follows: $\lg(N) = a + b\lg(S_{\max} - A)$, where a, b are the material constants, $b<0$, and A is the theoretical fatigue limit stress amplitude. The S-N curves are shown in Fig.5 and the fatigue limits are shown in Fig.6.

Fig.5 and Fig.6 show that the aging temperature has great effects on the HCF life of 7075 aluminum alloy, with decreasing stress and increasing life. The fatigue life has great dispersion even under the same stress level and exceeds 10^7 under a certain stress level. After solution treatment (480 ℃ for 0.5 h), the fatigue life increases obviously under low stress level (>300 MPa), but decreases slightly under high stress level, the

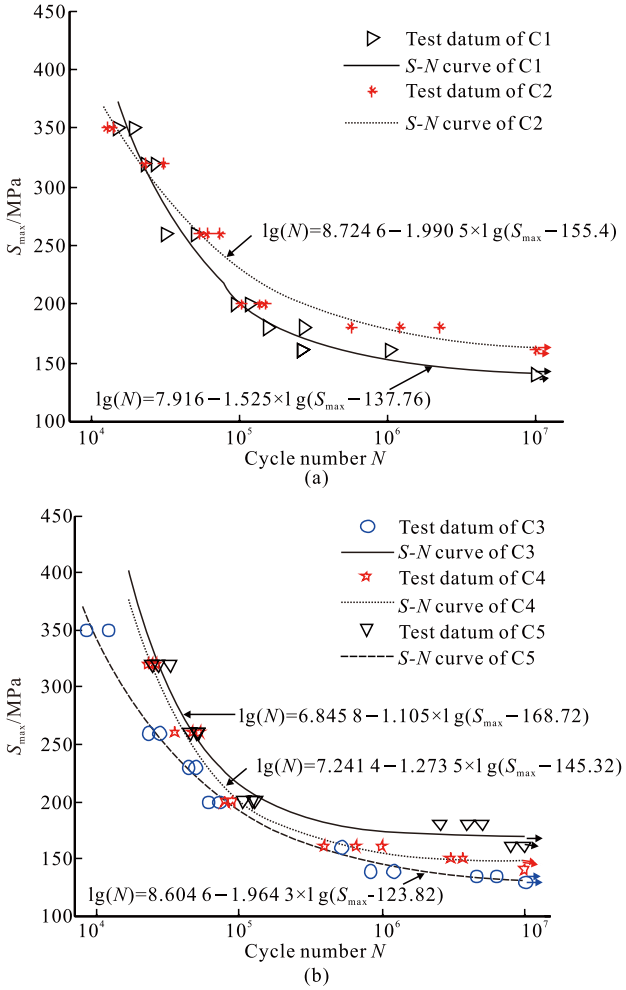

Fig.5 (a) The *S-N* curves of the test C1 and the test C3; (b) the S-N curves of the test C3-C5

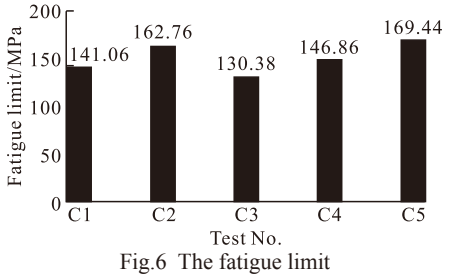

Fig.6 The fatigue limit

fatigue limit increased from 141.06 to 162.76 MPa, the results show that the solution treatment can improve the fatigue limit. With the increase of aging temperature, the fatigue life of 7075 aluminum alloy increases obviously. The fatigue limit is 130.38 MPa after aging at 150 ℃ for 10 h and 146.86 MPa after aging at 170 ℃ for 10 h, while aging at 190 ℃ for 10 h, the fatigue limit is up to 196.44 MPa. The results suggest that the aging treatment can improve the fatigue performances to a certain extent and in the range of 150-190 ℃, the HCF performances of 7075 aluminum alloy can be improved when the aging temperature increases.

4 Fatigue fracture morphology observation

4.1 Fatigue crack initiation

The fatigue fracture surfaces of tests C3-C5 under 260 MPa were observed by scanning electron microscopy (SEM). Fig.7 shows the overall fracture surfaces and the fatigue crack initiation. The fractographies consist of several different zones (Figs.7 (a), 7 (c), 7 (e)), including fatigue crack initiation (I), fatigue crack propagation (Ⅱ, slow propagation and fast propagation) and final fracture (III).

As is shown in the studies[19,20], for the specimens without internal tissue defects, the fatigue crack is often initiated by the stress concentration of the surface or subsurface. There are many factors leading to stress concentration, such as the defects (the small porosity and the surface scratches), and the impurities generated during the process of smelting and heat treatment. In these experiments, the crack initiates from the impurity phase particles detached from the matrix under the cyclic loading. The EDS results show that the compositions of those particles are the high silicon compounds and the rich iron metal compounds, as is shown in Figs.7 (g) and 7 (h).

The mechanical properties (Young's modulus, Poisson's ratio and strength) of the impurity phase particles are different from that of the alloy matrix. Under cyclic loading, the impurity phase particles slide and separate from the matrix (high silicon phase) or fracture themselves (rich iron phase), then the crack appears at the weak point of the critical location and propagates from the initiation to the inward along the direction of perpendicular loading, then the fatigue crack propagation is formed. Because the fatigue crack initiation surfaces are exposed to the air, the propagations rate is slow. Repeating open and close cyclic loading makes the fracture surface smooth and bright. Meanwhile, those cracks initiated at different plane meet during propagation, the radial stairs are left, as shown in Figs.7 (b), 7 (d), 7 (f).

4.2 Fatigue crack propagation

The SEM morphologies of fatigue crack propagation regions under 260 MPa are shown in Fig.8. The fatigue crack propagation includes two stages: after crack initiates, the cracks propagate along the primary slip plane of the slip band to the inside of metal by pure shear way, forming the first stage of fatigue crack propagation, which is shown in Figs.8 (a), 8 (c) and 8 (e). When the crack propagates a certain length, the

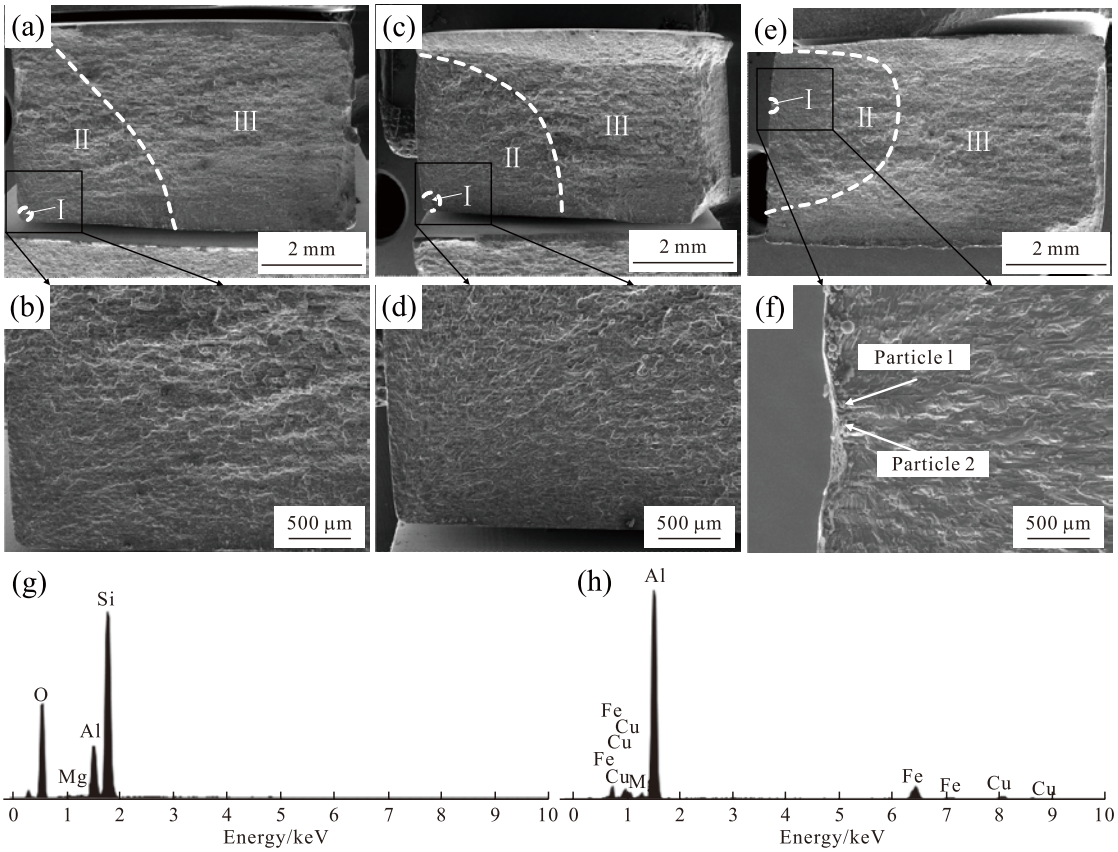

Fig.7 Fatigue-fractured surface and the morphology of the fatigue initiation of 7075 aluminum alloy treated at different aging temperature: (a) fatigue-fractured surface of the test C3; (b) fatigue initiation morphology of the test C3; (c) fatigue-fractured surface of the test C4;(d) fatigue initiation morphology of the test C4;(e) fatigue-fractured surface of the test C5;(f) fatigue initiation morphology of the test C5;(g) EDS of particle 1; (h) EDS of particle 2

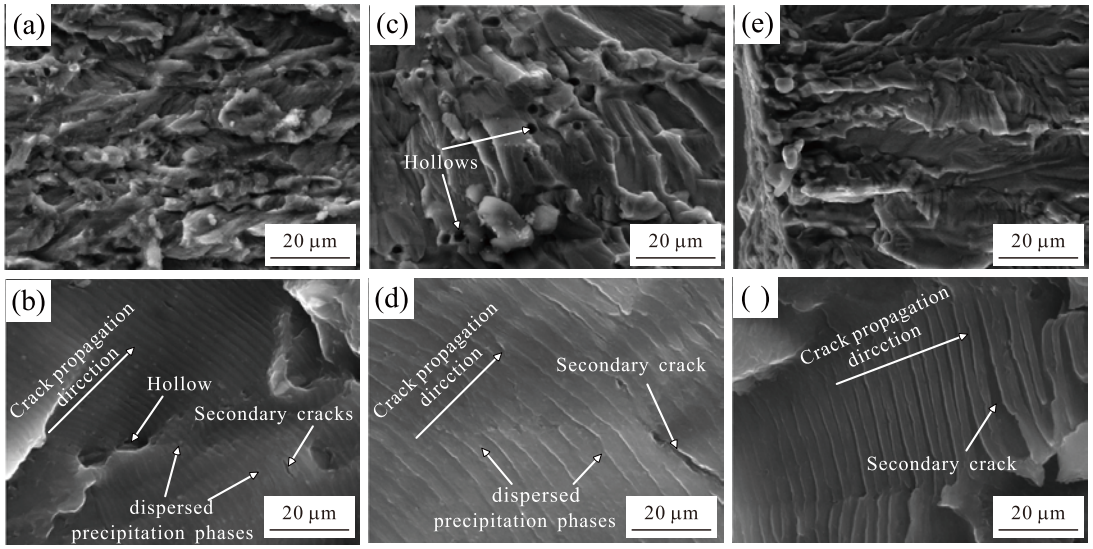

Fig.8 Fatigue crack propagation morphology of 7075 aluminum alloy treated at different aging temperature: (a) morphology of test C3; (b) fatigue stripes of test C3; (c) morphology of test C4; (d) fatigue stripes of test C4; (e) morphology of test C5; (f) fatigue stripes of test C5

direction is changed, the crack propagates along the perpendicular direction of the stress, the second stage of fatigue crack propagation appears, which is shown in Figs.8 (b), 8 (d) and 8 (f).

As is shown in Figs.8 (a), 8 (c) and 8 (e), the quasi-cleavage fracture plane and the parallel zigzag section are observed on the fractographies of 7075 aluminum alloy which is aged at different temperature. After aging treatment, abundance of nano strengthening phases exit in the matrix, the crack propagation

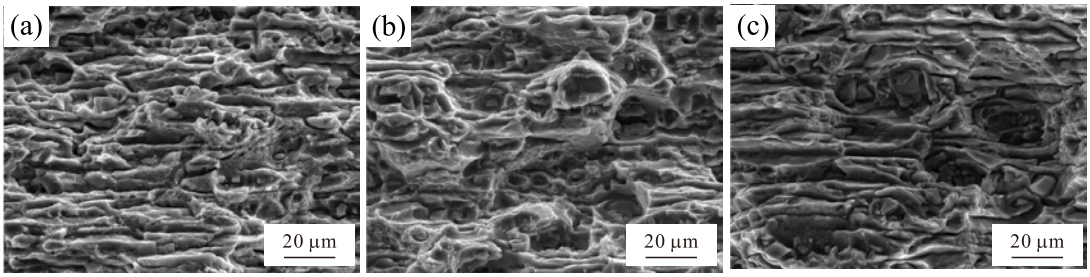

Fig.9 Final fracture morphologies of 7075 aluminum alloy treated at different aging temperature: (a) test C3; (b) test C4; (c) test C5

is blocked and large deformation appears on the boundaries of cracks, leading to the cracks merging by tearing them and resulting in forming lamella fracture surface. The quasi-cleavage fracture plane's area of test C3 (aged at 150 ℃ for 10 h) is the smallest, while the quasi-cleavage fracture plane's area of test C4 is the largest. The shape and size of quasi-cleavage fracture plane are associated with the microstructure of the alloy (the grain size, the precipitated phase type, size and distribution), the larger the grain, the larger the quasi-cleavage fracture plane's area.

The fatigue strips can be observed in the second stage of the fatigue crack propagation. Each strip represents a stress cycle and shows the location of the crack tip under this cycle, as is shown in Figs.8 (b), 8 (d) and 8 (f). The average widths of test C3 (aged at 150 ℃ for 10 h), test C4 (aged at 170 ℃ for 10 h), and test C5 (aged at 190 ℃ for 10 h) are 0.32, 0.77 and 0.4 μm respectively. Some second micro cracks parallel to the strips are observed on the fatigue crack propagation surfaces. The crack propagation is blocked by the second phase particles and the propagation direction is changed, eventually, the crack goes around them and continues propagating. Under the cyclic loading, the second phase particles desquamate from the matrix and the holes are left[21]. The diameter of the second phase particles is 2 μm to 3 μm by measuring the size of the holes, which have negative effects on HCF performance. Furthermore, there are many nanoscale precipitated phase particles dispersed in the matrix, which have positive effects on HCF performance.

4.3 Final fracture

When the crack length reaches the critical size, the material fails to bear the cyclic loading, the crack propagation becomes unstable and finally the meaterial fractures transiently. The SEM images of the final facture are shown in Fig.9.

It can be seen from Fig.9 that the surfaces of the final facture are coarse and mixed ductile-brittle fracture with many tearing ridges. The dimple number of test C3 (aged at 150 ℃ for 10 h) is the least and the size is the smallest. The results show that the dimple size and depth of 7075 aluminum alloy increase gradually with the increase of aging temperature. The number of dimples is in close relationship with the precipitated phase particles. The more and the finer precipitated phase particles, the more the dimples. It can be deduced that with the increase of aging temperature, a lot finer predicated phase particles appear.

5 Conclusions

a) The 7075 aluminum alloy under the temper T651 shows the best mechanical performances (hardness: 200 HV, tensile strength: 585.3 MPa, 0.2% offset yield strength: 519.0 MPa); the solution treatment (treatment at 480 ℃ for 0.5 h) reduces the mechanical performances, but the aging treatment improves the mechanical performance. With increasing aging temperature (aged at 150-190 ℃ for 10 h), the mechanical performances (hardness, tensile strength, 0.2% offset yield strength, elongation) decrease firstly and then increase, the peak value appears at 190 ℃, respectively, 187 HV, 569.6 MPa, 505 MPa, 12.6%.

b) Under high stress condition, the life of 7075 aluminum alloy after solution treatment is lower than the life of temper T651, but higher than the temper T651 under low stress condition. The aging temperature has a significant effect on the HCF performance. With increasing aging temperature (150 ℃-190 ℃), the HCF life increases. The fatigue limits are estimated for 130. 06, 146.86, and 169.44 MPa respectively.

c) The fracture morphologies and EDS show that the crack initiate from the impurity particles (the high silicon and rich iron metal compounds) of the subsurface, and the crack propagation is a kind of ductile-brittle mixed fracture. With increasing aging temperature, the area of quasi-cleavage planes and the width of fatigue strips increase first and then decrease, the maximum values appear at 170 ℃; The final fracture regions have the characteristics of dimple, with

increasing aging temperature, the size becomes bigger and the depth becomes deeper.

References

[1] Zhu A W, Starke E A. Materials Aspects of Age-Forming of Al-*x*Cu Alloys[J]. *Journal of Materials Processing Technology*, 2001, 117(3): 354-358

[2] Inforzato D J, Costa J P R, Fernandez F F, *et al.* Creep-Age Forming of AA7475 Aluminum Panels for Aircraft Lower Wing Skin Application[J]. *Materials Research*, 2012, 15(4): 596-602

[3] Cheng W. Application of Advanced Aluminum Alloys in A380 Structures[J]. *Aviation Maintenance & Engineering*, 2005, 50(2): 41-47

[4] Adachi T, Kimura S, Nagayama T, *et al.* Age Forming Technology for Aircraft Wing Skin[C]. *Materials Forum*, 2004

[5] Sarioğlu F, Orhaner F Ö. Effect of Prolonged Heating at 130 ℃ on Fatigue Crack Propagation of 2024 Al Alloy in Three Orientations[J]. *Materials Science and Engineering: A*, 1998, 248(1): 115-119

[6] Bray G H, Glazov M, Rioja R J, *et al*. Effect of Artificial Aging on the Fatigue Crack Propagation Resistance of 2000 Series Aluminum Alloys[J]. *International Journal of Fatigue*, 2001, 23(1): 265-276

[7] Jin X, Wan M, Li C. Effect of Creep Age Forming on Fatigue for 7B04 Aluminum Alloy[J]. *Forging & Stamping Technology*, 2011, 36(2): 124-127

[8] Zhan L H, Li Y U, Huang M H. Microstructures and Properties of 2124 Alloy Creep Ageing under Stress[J]. *Journal of Central South University (Science and Technology)*, 2012, 43 (3): 926-931

[9] Zhu A W, Starke E A. Stress Aging of Al-*x*Cu Alloys: Experiments[J]. *Acta Materialia*, 2001, 49(12): 2 285-2 295

[10] Liu J H, Li D, Liu P Y, *et al*. Effect of Ageing and Retrogression Treatments on Mechanical and Corrosion Properties of 7075 Aluminum Alloy[J]. *Transactions of Metal Heat Treatment*, 2002, 23(1): 50-54

[11] Zhu C C, Luo J Y. Stretch Rate and Deformation for Pre-stretching Aluminum Alloy Sheet[J]. *Journal of Central South University*, 2012, 19(4): 875-881

[12] Zhan L H, Li Y G, Huang M H. Effect of Process Parameters on Microstructures of 7055 Aluminum Alloy in Creep Age Forming[J]. *Applied Mechanics and Materials*, 2011, 80(1): 40-45

[13] ASTM. *Tension Testing of Metallic Materials (Metric)*[S]. ASTM E8M-04, 2004

[14] ASTM. *Standard Practice for Conducting Force Controlled Constant Amplitude Axial Fatigue Tests of Metallic Materials*[S]. ASTM E466, 2007

[15] Yin Z P. *Structural Fatigue and Fracture*[M]. Shanxi: Northwestern Polytechnical University Press, 2012

[16] Chen C Y. *Fatigue and Fracture*[M]. Wuhan: Huazhong University of Science and Technology Press, 2005

[17] Basquin O H. The Exponential Law of Endurance Tests[C]. *Proc. ASTM,* 1910

[18] Weibull W. *Fatigue Testing and Analysis of Esults*[M]. London: Pergamon Press, 1961

[19] Cui Y X, Wang C L. *Metal Fracture Analysis*[M]. Harbin: Harbin Industrial University Press, 1998

[20] Liu X L, Zhang Z, Tao C H. *Fatigue Fracture Quantitative Analysis*[M]. Beijing: National Defense Industry Press, 2010

[21] Srivatsan T S. An Investigation of the Cyclic Fatigue and Fracture Behavior of Aluminum Alloy 7055[J]. *Materials & Design*, 2002, 23(2): 141-15